KSME

Springer

Journal of Mechanical Science and Technology 35 (2) 2021

Original Article
DOI 10.1007/s12206-021-0127-x

Keywords:
· Angular contact ball bearings
· Dynamic stiffness
· Thermal characteristics
· Thermal-mechanical coupling

Correspondence to:
Xuanyu Sheng
xuanyu@tsinghua.edu.cn

Citation:
Wang, L., Sheng, X., Luo, J. (2021). Thermal-mechanical fully coupled analysis of high-speed angular contact ball bearings. Journal of Mechanical Science and Technology 35 (2) (2021) 669~678. http://doi.org/10.1007/s12206-021-0127-x

Received August 9th, 2020
Revised November 2nd, 2020
Accepted November 9th, 2020

† Recommended by Editor Seungjae Min

Thermal-mechanical fully coupled analysis of high-speed angular contact ball bearings

Lanwen Wang, Xuanyu Sheng and Jianbin Luo

Department of mechanical engineering, Tsinghua University, Beijing 100084, China

Abstract The thermal and mechanical properties of angular contact ball bearings are critical to their operating accuracy and service life. On the basis of the theory of dynamics and frictional heat generation, this work establishes a thermal-mechanical fully coupled model. The high-speed motion characteristics, temperature, and dynamic stiffness are analyzed, and the simulation results are compared with the theoretical calculation and experimental results. Then, the temperature and axial deformation of the bearings under different rotation speeds are analyzed, and the laws of mechanical and thermal characteristics of the bearings are obtained. Results show that an increase in the rotation speed of the inner ring causes the temperature of each component to increase, with the contact area of the balls showing the greatest increase in temperature. An increase in rotation speed also increases the axial deformation of the inner ring.

1. Introduction

High-speed angular contact ball bearings are widely used in important fields, such as aviation, railways, and precision equipment. Their performance and geometric design have received great attention, and their bearing capacity and dynamic characteristics directly affect fatigue life, temperature rise, and stability [1-3]. The heat generation problem caused by the high-speed operation of bearings seriously affects bearing performance. If the frictional heat inside a bearing cannot be dissipated in time, then the operating temperature of the bearing increases. An excessive temperature rise causes a series of problems, such as flashback or burns on the raceway and rolling elements, lubricant failure, and reduced load capacity; these problems lead to the early scrapping of bearings [4]. Therefore, analyzing the thermal characteristics and mechanism of bearings and accurately predicting their temperature distribution are key issues in the research of high-speed rolling bearings.

At present, the numerical analysis methods for rolling bearings are mainly divided into two categories. The first category focuses on the analysis of the mechanism of the thermal characteristics of bearings, including heat generation and heat dissipation. The most widely used method is the thermal network method, which is based on the theory of thermal resistance. In this method, the research object is divided into multiple unit nodes, and heat transfer is established according to Kirchhoff's current law and Kirchhoff voltage law. This method initially analyzes the statics and kinematics of a bearing on the basis of Harris bearing theory [5, 6]. After iteratively solving the bearing speed, contact load, and other parameters, the method calculates the bearing heat generation according to the local method or overall method. The overall method multiplies the overall friction torque and speed to find the overall power consumption of the bearing; the empirical formula proposed by Palmgren is commonly used [7]. Based on the kinematic relationship of bearings, the local method separately obtains the local friction power consumption of each contact part of a bearing and sums them up to obtain the total power consumption. Thereafter, the thermal network is established for bearing heat transfer analysis, and the temperature of each component is obtained by solving the heat equilibrium equation.

Zheng De-xing et al. proposed a multinode planning scheme for rolling bearings and established a thermal network to analyze the thermal characteristics of high-speed angular contact ball bearings [8, 9]. Later, the Gauss-Seidel method was used to solve the heat equilibrium equation, and the thermal network model was optimized [10]. Takabi et al. established a thermal network model with 17 thermal nodes and used the explicit Runge-Kutta method to solve the thermal equilibrium equation; they subsequently obtained the transient temperature distribution of the bearing [11]. He considered the thermal expansion and centrifugal expansion of a bearing and established a thermal network model with seven nodes; then, they analyzed the influence of thermal expansion and centrifugal expansion on bearing characteristics [12]. Yan et al. established a transient thermal network model and compared the accuracy of the overall method and local method in calculating heat generation [13]. Zahedi et al. proposed a transient thermal network model of bearings and spindle system and analyzed the temperature distribution of the spindle system [14].

The second category involves establishing a finite element model (FEM) to simulate the temperature field distribution and thermal deformation of bearings. It includes static analysis, quasistatic analysis, quasidynamic analysis, and dynamic analysis. At present, the commonly used method is to calculate the theoretical heat generation of a bearing through an empirical formula, establish an FEM, and apply a heat source to analyze the transient and steady-state temperature distribution of the bearing. Wang et al. established a transient thermal analysis FEM of a bearing and spindle system and combined it with boundary conditions and thermal feedback of thermal contact conductance to estimate thermal characteristics in real time [15]. Ye et al. established an FEM of a high-speed angular contact ball bearing, conducted thermal analysis, and optimized the geometric parameters according to the radial thermal expansion of the bearing; subsequently, the bearing characteristics and fatigue life of the bearing were analyzed [16]. Than et al. established a two-dimensional FEM of a high-speed bearing and spindle system and corrected the heat generation parameters according to the experimentally measured two-point temperature [17]. Through finite element thermal analysis and a multiobjective optimization model, Cui et al. optimized the radial clearance and preload of a bearing, with stiffness and temperature rise as the objective functions [18]. Yan et al. ignored the cage and calculated frictional heat by using the local method; then, they established the sequential coupling FEM of the bearing and analyzed the temperature field distribution [19]. On the basis of the multipoint experimental temperature data collected from a ball bearing, a multiobjective optimization model was established to modify the heat transfer parameters of the bearing, and the thermal elongation of the bearing and spindle system was analyzed [20]. Ma et al. considered the influence factors of boundary conditions, such as the morphology and thermal contact resistance of rough surfaces, and established an FEM for the thermal characteristic analysis of high-speed spindle systems [21].

At present, the existing methods still suffer from a number of problems. The thermal network method is constrained by the number of nodes, and the temperature distribution inside each component cannot be obtained. In addition, the motion state of bearings under high-speed operation is complex, and the influence factors of heat generation and heat transfer are complicated. Therefore, many scholars have modified the coefficients in the empirical formula to close the gap between the temperature calculation results and the experimental results; however, doing so is relatively difficult [22]. The current finite element method involves applying a fixed or moving heat source without considering the motion and dynamic characteristics of bearings and without simulating the motion state and heat generation process of bearings. Therefore, simulation results greatly different from actual situations. In addition, the current FEM of bearing thermal analysis is mostly sequential coupling. Therefore, a fully coupled model is currently lacking. To solve these existing problems, the current work establishes a thermal-mechanical fully coupled FEM of high-speed angular contact ball bearings on the basis of the theory of dynamics and frictional heat generation. The proposed model comprehensively considers the effects of thermal and mechanical loads. The results of the coupling analysis of high-speed motion characteristics, frictional heat generation characteristics, heat transfer characteristics, and thermal expansion characteristics of bearings and the simulation results are compared with the experimental and theoretical calculation results. After the verification of the proposed model, the temperature and axial displacement field of bearings under different working conditions are analyzed to obtain the laws of mechanical and thermal characteristics of bearings under high-speed operation.

2. Methodology

The centrifugal force and gyroscopic moment of angular contact ball bearings are important factors during high-speed operation and cannot be ignored. Therefore, dynamic analysis is required. At the same time, a strong coupling exists between the mechanical and thermal characteristics of rolling bearings under high-speed operating conditions. This feature requires a thermal-mechanical fully coupled analysis. Fully coupled analysis considers the interaction of heat and machinery in real time and can thus accurately characterize the running state of bearings.

2.1 Basic theory

This section introduces the equilibrium equation of thermal-mechanical coupling and the theoretical calculation method for bearing motion for comparison with finite element results. The calculation methods for bearing heat generation and heat transfer coefficient are subsequently introduced.

2.1.1 Equilibrium equation

The equilibrium equations for dynamic analysis and thermal analysis in the finite element method are

$$[M]\{\ddot{u}\}+[C]\{\dot{u}\}+[K]\{u\}=[P] \tag{1}$$

$$\left[C(T)\right]\left\{\dot{T}\right\}+\left[K(T)\right]\{T\}=\left[Q(T)\right] \tag{2}$$

where [*M*] is the mass matrix, [*C*] is the damping matrix, [*K*] is the stiffness matrix, [*P*] is the load vector, [*C*(*T*)] is the specific heat matrix, [*K*(*T*)] is the heat transfer matrix, [*Q*(*T*)] is the heat flow load vector, *u* is the displacement component, and *T* is the temperature. These equations are generally solved by the explicit integration method.

$$\begin{cases} \dot{u}^N_{\left(i+\frac{1}{2}\right)}=\dot{u}^N_{\left(i-\frac{1}{2}\right)}+\dfrac{\Delta t_{(i+1)}+\Delta t_{(i)}}{2}\ddot{u}^N_{(i)} \\ u^N_{(i+1)}=u^N_{(i)}+\Delta t_{(i+1)}\dot{u}^N_{\left(i+\frac{1}{2}\right)} \end{cases} \tag{3}$$

$$T^N_{(i+1)}=T^N_{(i)}+\Delta t_{(i+1)}\dot{T}^N_{(i)} \tag{4}$$

where *i* is the increment. The displacement component uses the central differential integration rule, and the temperature uses the forward differential integration rule. This method includes inertial effects and can simulate the transient thermal response. Hence, it is suitable for the analysis of high-speed angular contact ball bearings. In the analysis, the temperature distribution and thermal deformation are calculated, thus affecting the stress analysis. At the same time, the stress distribution affects the temperature solution so as to achieve full coupling.

2.1.2 Kinematic analysis

The kinematic relationship of bearings needs to be analyzed to accurately analyze the friction heat generation process of angular contact ball bearings. Rolling ball bearings under high-speed conditions are mostly controlled by outer ring raceways due to centrifugal force. Therefore, in the theoretical solution process, the theory of outer ring raceway control is adopted; that is, the ball is assumed to roll purely on the outer raceway without spinning. During the operation of a bearing, the gyro rotation is considerably small. In the case in which gyro movement is ignored, the calculation formula for the ball rotation angular velocity ω_m for a bearing with a fixed outer ring and rotating inner ring is

$$\omega_m=\frac{1-\gamma\cos\alpha_i}{1+\cos(\alpha_i-\alpha_o)}\omega,\quad \gamma=\frac{D_b}{d_m} \tag{5}$$

where D_b is the diameter of the ball; d_m is the pitch diameter; α_i, α_o are the actual contact angles of the ball with the inner and outer raceways, respectively; and ω is the angular velocity of the inner ring. The actual contact angles of the ball with the inner and outer raceways are obtained by the load analysis of a single ball and the entire bearing. The solution flowchart is shown in Fig. 1. After listing the equilibrium equations of a single ball and the entire bearing, the actual contact angle and contact load can be iteratively solved by the Newton-Raphson method. The ball revolving angular velocity can then be obtained and compared with the finite element calculation model.

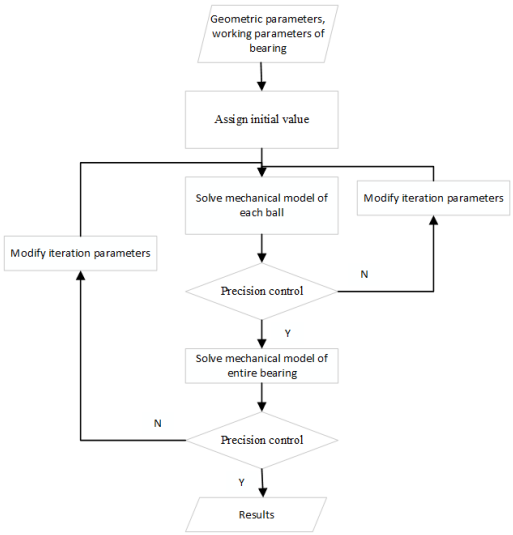

Fig. 1. Flowchart of bearing mechanics analysis.

2.1.3 Heat generation

When the bearing is running at a high speed, the friction energy dissipation rate of the contact area is

$$P_f=\boldsymbol{\tau}\cdot\dot{\boldsymbol{\gamma}} \tag{6}$$

where $\boldsymbol{\tau}$ is the frictional stress; $\dot{\boldsymbol{\gamma}}$ is the slip rate; and the frictional heat generated by the two contact surfaces are

$$q_1=f\eta P_f,\qquad q_2=(1-f)\eta P_f \tag{7}$$

where *f* is the proportion of frictional heat flowing into the first surface and η is the coefficient of the conversion of mechanical energy into thermal energy. Friction stress depends on friction coefficient and contact stress. Rolling bearings are in point-contact elastohydrodynamic lubrication under high-speed operation. Therefore, the bearing operating speed should be calculated in conjunction with bearing kinematics theory, and the specific friction coefficient should be determined through elastohydrodynamic lubrication [23, 24]. In the current work, the coefficient of friction is calculated through the coupling of thermo-elastohydrodynamic and bearing dynamics. The calculation flowchart is shown in Fig. 2.

2.1.4 Heat dissipation

The heat in the bearing is mainly transferred by means of heat conduction and heat convection. Heat conduction is calculated according to Fourier's law, and the thermal conductivity of

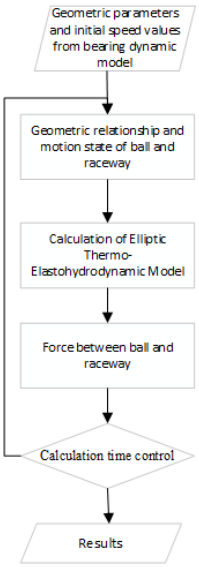

Fig. 2. Flowchart of thermo-elastohydrodynamic and bearing dynamics coupling.

each components is easily obtained. The determination of the convective heat transfer coefficient h in thermal convection calculation is relatively complicated, and it is affected by a variety of complex factors. At present, the commonly used determination methods are the analytical method, experimental method, comparison method, and numerical method. Harris proposed a calculation model for the convective heat transfer coefficient of rolling bearings on the basis of laminar flow assumption [5]. The calculation formula of forced convection heat transfer coefficient between the bearing and the lubricant is

$$h = 0.332 \frac{k}{d_m} P_r^{\frac{1}{3}} R_e^{\frac{1}{2}} \tag{8}$$

where k is the thermal conductivity of the lubricant, P_r is the Prandtl number of the lubricant, $R_e = \frac{u_s x}{v_0}$ is the Reynolds number, u_s is the surface speed of the cage, and v_0 is the kinematic viscosity of the lubricating oil. The convective heat transfer coefficient between the outer surface of the bearing and the air is

$$h = \begin{cases} 2.3\times10^{-5}(T - T_a)^{0.25} & \text{Natural convection} \\ 0.03 \frac{k_a}{D_o} R_e^{0.57} & \text{Forced convection} \end{cases} \tag{9}$$

In still air, the form of convection is natural convection. T_a is the ambient temperature. In flowing air, the form of convection is forced convection. k_a is the thermal conductivity of air, D_o is the outer diameter of the bearing, $R_e = \frac{u_a D_o}{v_a}$, u_a is the flow velocity of air, and v_a is the kinematic viscosity of air.

Table 1. Structural parameters of 7008CETA.

Symbol	Parameter	Value
D_o/mm	Outer diameter	68
D_i/mm	Inner diameter	40
B/mm	Width	15
d_m/mm	Pitch diameter	54
D_b/mm	Diameter of ball	7.938
Z	Number of balls	18
α/°	Contact angle	15
d_o/mm	Outer ring raceway diameter	61.949
d_i/mm	Inner ring raceway diameter	46.034
r_o/mm	Radius of curvature of outer raceway groove	4.125
r_i/mm	Radius of curvature of inner raceway groove	4.375

Table 2. Grid parameters of 7008CETA.

Part	Number of nodes	Number of elements
Inner ring	7210	5670
Outer ring	10682	8428
Cage	3006	1818
Balls	70722	62208

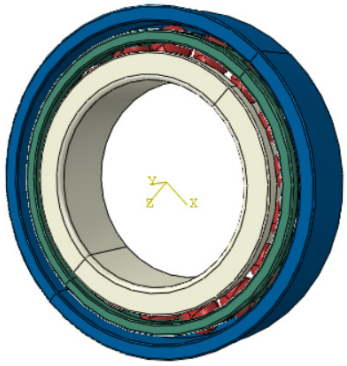

Fig. 3. Finite element model of 7008CETA.

2.2 Finite element model

The structural parameters of 7008CETA angular contact ball bearings are shown in Table 1. When establishing the FEM, chamfers, fillets, and other small geometrical bodies with little influence on the analysis are ignored. The model is shown in Fig. 3, and the grid parameters are shown in Table 2.

The material of the main structure (inner ring, outer ring, balls) is GCr15Z, and the material of the cage is phenolic tape. The mechanical and thermodynamic performance parameters of the two materials at room temperature are shown in Table 3.

The following assumptions and simplifications are made in the model to facilitate analysis. (1) The surface heat transfer coefficients between each contact body of the bearing are difficult to determine. They are related to the thermal conductivity of each body and the rotation speed of the bearing. Hence, the average thermal conductivity of the two contacting bodies is

Table 3. Material parameters.

Material	GCr15Z	Phenolic tape
Density (kg/m^3)	7800	1800
Elastic modulus (GPa)	207	2.6
Poisson's ratio	0.30	0.35
Thermal conductivity (W/(m*K))	30	0.72
Specific heat (J/(kg*K))	450	1500
Thermal expansion coefficient (°C^{-1})	1.15*10^{-5}	1.98*10^{-5}

Table 4. Lubricant parameters.

Type	Viscosity of base oil (cSt)		Cone penetration (1/10 mm)	Dropping point (°C)
	40 °C	100 °C		
L252	25	6	250-265	250

approximately taken in the analysis. (2) The assumption is that parameters such as friction coefficient and thermal expansion coefficient do not change with changes in temperature and stress and that they are constant throughout the analysis process. The friction coefficient and convection heat transfer coefficient are related to the lubricant. The bearing uses L252 grease, and its parameters are shown in Table 4.

The rolling friction coefficient of the bearing is calculated to be 0.03 according to the theory of thermo-elastohydrodynamic lubrication. The convective heat transfer coefficient between the bearing and the grease is calculated to be 80 W/(m^2*°C) according to the convection heat transfer formula. The surface heat transfer coefficient between the ball and inner ring and the ball and outer ring contact pair is 30 W/(m*K), and the surface heat transfer coefficient of the ball and cage contact pair is 15 W/(m*K). Assume that the coefficient of the conversion of mechanical energy into thermal energy of a friction pair is 1 and that the proportion of friction heat flowing into both contact surfaces is 50 %. The inner ring of the bearing rotates, and the outer ring is fixed. During the simulation, an axial load of 350 N is applied to the inner ring, and a rotation speed of 0-12000 rpm is applied to the inner ring. The speed increasing process adopts a smooth curve, and it continues to run after reaching the maximum speed until the ball rotates steadily. The ambient temperature and the initial temperature of each component of the bearing are both 20 °C. The temperature field distribution in the analysis step is then calculated by the Abaqus/Explicit solver as the bearing rotates. The element type of all components adopts C3D8RT (eight-node entity reduced-integration element, with T indicating thermal degrees of freedom).

2.3 Experimental setup

Verifying the accuracy of the finite element simulation model requires a high-speed bearing performance test. The test uses the angular contact ball bearings and lubricants used in the finite element analysis and builds a shaft system. The structure of the test shaft system is shown in Fig. 4, and the physical picture of the experimental equipment is shown in Fig. 5. Angular contact ball bearings are installed face to face, and an axial loading body structure is built on the right end to apply axial loads. A PT100 temperature sensor is inserted into the bearing seat to directly measure the temperature of the bearing's outer ring. A vibration sensor measures the vibration of the test head body. The shaft rotation accuracy is axial and radial ≤ 0.003 mm. The axial loading mode is hydraulic loading, and the test axial load is 350 N. The radial stiffness of the bearing support of both sides of the shaft is about 180 N/μm, and the test speed range is 12000-36000 rpm.

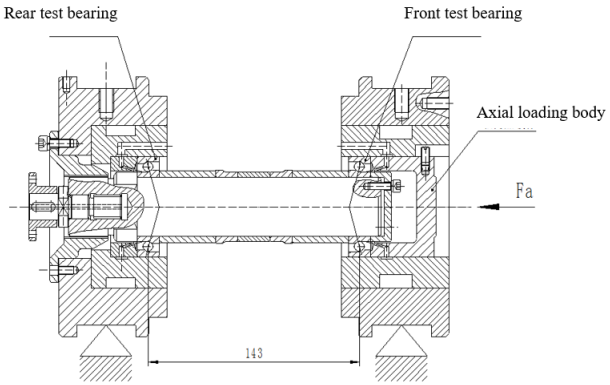

Fig. 4. Structure of test shaft system.

Fig. 5. Physical picture of experimental equipment.

3. Results

On the basis of the FEM established in the previous section, the motion speed, temperature field distribution, and axial and radial deformation of the bearing components are obtained after the calculation is completed. At the same time, the revolution speed of the ball is obtained through theoretical calculation, the temperature of the outer ring of the bearing is obtained through the test, and the accuracy of the FEM is verified by comparison.

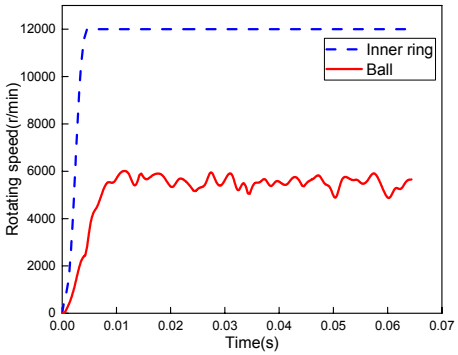

Fig. 6. Rotation speed variation curve with time.

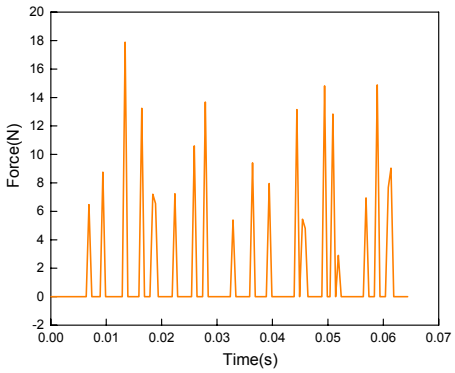

Fig. 7. Collision force between the ball and the cage.

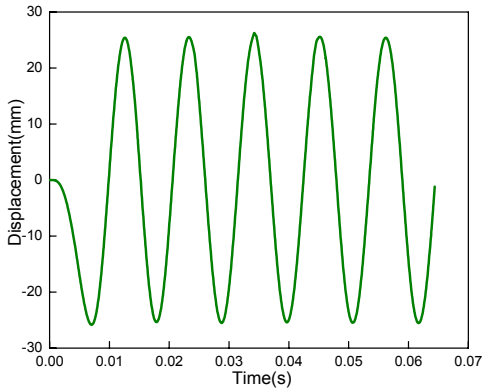

(a) X-direction displacement

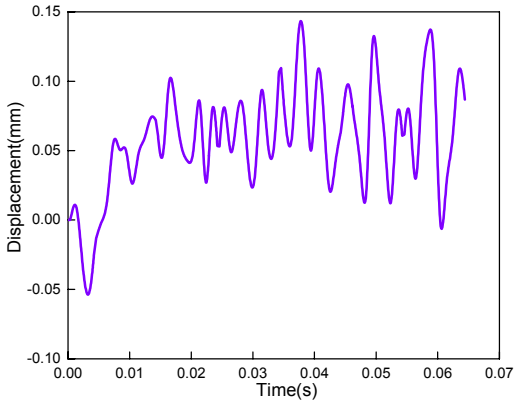

(b) Y-direction displacement

Fig. 8. Displacement of balls.

3.1 Motion analysis

Ball motion must be analyzed prior to evaluating the frictional heat generation of the bearing. Fig. 6 shows the changes of speed with time of the inner ring and ball according to the calculation.

According to the simulation results, the average revolving speed of the ball is 5012 rpm. According to the kinematics theory solution, the revolving speed of the ball is 5187 rpm. The relative error between the two results is 3.37 %. Thus, the motion condition solved by the FEM is accurate. In the dynamic simulation, only the inner ring is set to rotate, and the cage is not constrained in any direction of freedom. When the bearing is running, the inner ring drives the rolling element and then drives the cage to rotate. In this way, the vibration of the inner ring and cage in all directions and the repeated collision between the cage and the rolling body reduce the revolution speed of the ball and cage. The real-time collision force between the ball and the cage is shown in Fig. 7. In addition, the axis of rotation is not fixed during operation, and the degrees of sway in all directions differ. Hence, the output speed not a straight line. However, macroscopically, the angular velocity of the ball tends to be stable. The center node of the ball is selected, and the displacement curve in the X- and Y-directions of the global coordinate system is plotted, as shown in Fig. 8.

As shown in the figure, the overall movement of the ball in the X-direction is relatively stable and has obvious periodicity. The maximum displacement is 26.92 mm. As the pitch radius is 27 mm, the movement in the X-direction conforms to the actual situation. Vibration occurs in the movement of the ball in the Y-direction. At first, axial load is applied, and the axial displacement of the ball is negative.

After the bearing runs normally, the axial displacement of the ball is positive and vibrates continuously. The causes of vibration mainly include the following. (1) The gap between the cage and the ball. In the dynamics simulation, a gap exists between the cage pocket and the ball, and the cage has no constraints. Hence, the cage shakes in all directions during operation, and the collision between the cage and the inner ring causes the ball and cage to have irregular vibrations in all directions. (2) The influence of the grid. Simulating the running condition of the entire bearing requires a large amount of calculation. Given the limitations in time and computer configuration, the meshing cannot be divided finely. A large mesh size makes the surface of the rolling element and the raceway of the inner and outer rings rough. This condition results in an unstable operation and causes various levels of vibration in various parts of the model. (3) The elastic deformation and thermal deformation of the rolling element and inner ring also affect the axial displacement of the ball.

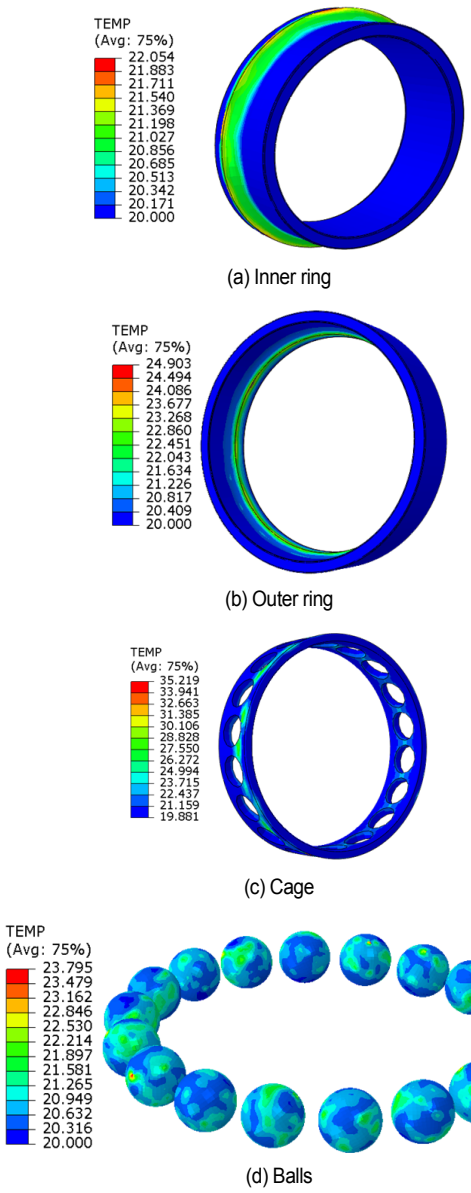

Fig. 9. Temperature distribution diagrams of bearing.

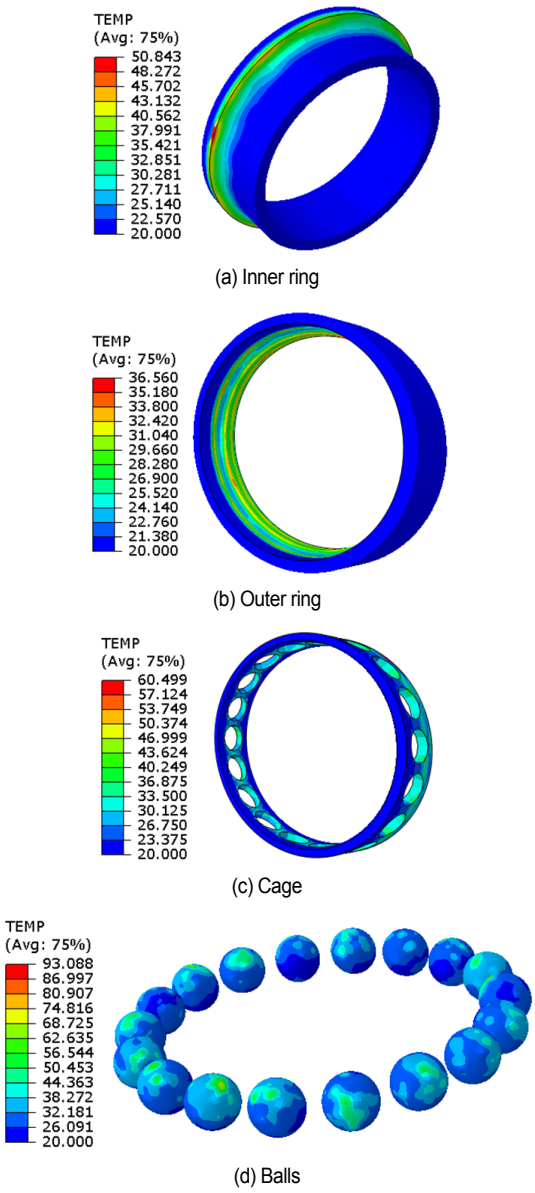

Fig. 10. Temperature distribution diagrams of bearing under 36000 r/min.

3.2 Temperature analysis

The temperature distribution of each component of the bearing is shown in Fig. 9. The temperature of the contact area of the bearing is higher than that of the noncontact area. The cage shows the largest temperature rise, followed by the outer ring, balls, and inner ring. The temperature of the local contact area is excessively high. Except for the cage, the temperature rise of all components is uniform, and the amplitude is small. The temperature distribution of the cage is not uniform, and a high local temperature occurs. This result is due to the facts that the cage is not a key component in the thermal analysis of the bearing; the meshing is relatively coarse; and the ball, inner ring, and outer ring collide during operation. According to the simulation results, the maximum temperature of the contact area of the bearing outer ring is 24.9 °C. The temperature of the bearing outer ring measured by the test is 23.9 °C, which is slightly lower than the simulated value. This result may be due to the temperature measured by the temperature sensor not being the maximum temperature of the outer ring. Overall, the simulated values are consistent with the experimental values, thus proving the accuracy of the thermo-mechanical fully coupling model.

4. Test and discussion

4.1 Effect of rotation speed on bearing temperature distribution

To study the effect of rotation speed on the bearing temperature distribution, this study calculates the temperature field of

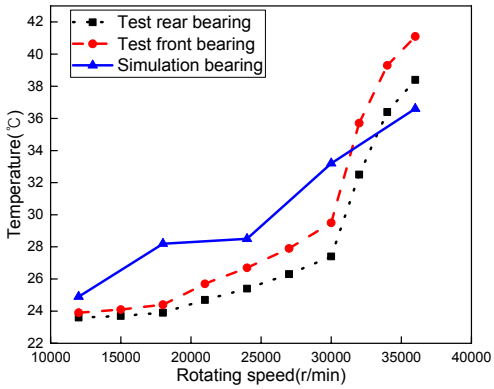

Fig. 11. Temperature change curve of outer ring with rotation speed.

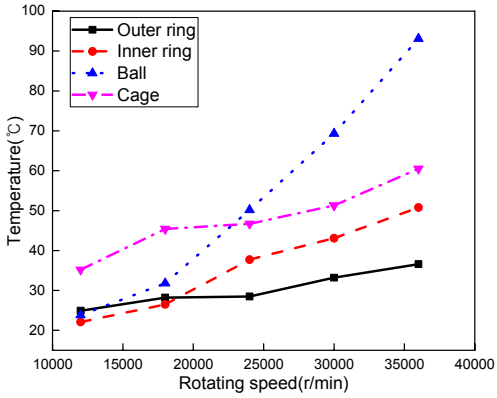

Fig. 12. Temperature change curve of each component with rotation speed.

the bearing components at different rotation speeds through simulation. The rotation speed of the inner ring is set to range from 12000 rpm to 36000 rpm, and thermal-mechanical fully coupling analysis is conducted. The temperature distribution of each component of the bearing under 36000 rpm is shown in Fig. 10. The change of the outer ring temperature with the rotation speed is compared with the experimental value. The result is shown in Fig. 11.

At low speeds, the simulation value of the temperature is higher than the experimental value. At 36000 rpm, the experimental value is higher than the simulation value. The maximum relative error is 14.3 %, and the minimum relative error is 4.6 %. Overall, the simulation values of the temperature are close to the experimental values. The causes of temperature errors may include the following. (1) Influence of the test shaft system. In the test, heat transfer occurs between the bearing and the shaft and between the bearing and the housing. Nevertheless, the simulation model is simplified, and only the overall heat transfer coefficient is set. (2) Influence of ambient temperature. The ambient temperatures in the test and simulation model may differ, and the ambient temperature may change during the test. (3) Accuracy of temperature sensor, installation location, and other factors.

The changes of the temperature of each component of the bearing with the rotation speed are shown in Fig. 12. The calculation results show that with the increase of the rotation speed, the temperature of each component increases. The temperature rises of the ball contact area is the largest and is thus consistent with the actual situation.

The reason is that the centrifugal force and gyroscopic moment of the ball increase under high-speed operating conditions. This condition increases the heat generation in the contact area, and the heat cannot be effectively dissipated. Under high-speed operating conditions, the temperature relationship of each component of the bearing is ball > cage > inner ring > outer ring. The motion of the ball is the most complicated as it includes revolution, rotation, and spin. Thus, the temperature of the contact area has the fastest rising trend. As the revolution speed of the ball is smaller than that of the inner ring, the angular velocity of the outer ring relative to the ball is quite small. Hence, the outer ring is less affected by frictional heat generation than the inner ring and ball. Therefore, the temperature rise of the outer ring contact area is smaller than that of the inner ring.

4.2 Effect of rotation speed on bearing dynamic stiffness

As a high-speed spindle bearing of the machine tool, its dynamic stiffness is of great importance. Under high-speed operating conditions, thermal expansion exerts an effect on the dynamic stiffness of the bearing. To analyze the decay mechanism of the dynamic stiffness of the bearing, this section analyzes the displacement field of the bearing inner ring, calculates the axial deformation and stiffness, and compares the result with the experimental outcomes. The axial displacement distribution of the inner ring is shown in Fig. 13.

The maximum axial displacement of the inner ring is 0.675 mm. Given the gap between the inner ring and balls and the outer ring and balls when the bearing is not loaded, rigid body displacement occurs after the axial load is applied. According to the displacement cloud diagram, the rigid body displacement of the inner ring is 0.243 mm. According to the maximum axial displacement minus the rigid body displacement, the axial deformation can be calculated as 0.432 mm. According to the experimental measurements, under this speed and load condition, the axial deformation is 0.4 mm, which is close to the simulation value. Therefore, the dynamic stiffness can be calculated as 810 N/mm.

The changes of the axial deformation of the bearing inner ring with the rotation speed are shown in Fig. 14. As the rotation speed of the inner ring increases, the axial deformation of the inner ring also gradually increases. The simulation value is greater than the test value at low speed, and the simulation value is less than the test value at high speed. The reason may be that the temperature field of the bearing affects the deformation of each component during the simulation, thereby affecting the axial displacement. In sum, the dynamic stiffness of the bearing decreases with the increase of the rotation speed. This condition affects the high-speed running state and accuracy of

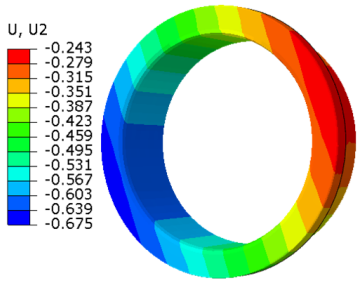

Fig. 13. Axial displacement distribution of inner ring.

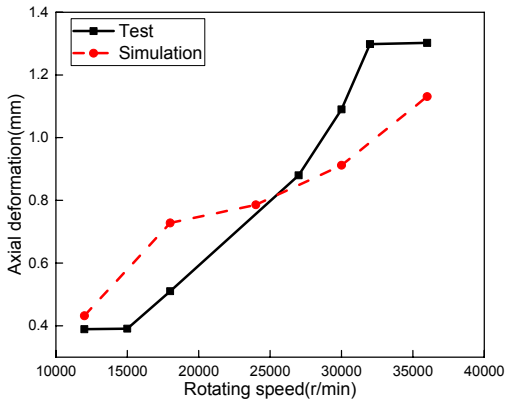

Fig. 14. Axial deformation change curve of inner ring with rotation speed.

the bearing and further influences the running state of the high-speed spindle system of the machine tool.

5. Conclusions

To analyze the thermal and mechanical characteristics of high-speed angular contact ball bearings, this study establishes a thermal-mechanical fully coupled FEM of high-speed angular contact ball bearings on the basis of the theory of dynamics and frictional heat generation. The high-speed motion characteristics, temperature field distribution, and dynamic stiffness of rolling bearings are analyzed. Then, the simulation results are compared with the theoretical calculation results and experimental results to verify the accuracy of the model. After the model is verified, the temperature and axial deformation of the bearing at different rotation speeds are analyzed to obtain the laws of mechanical and thermal characteristics of the bearing under high-speed operation. The new findings and main conclusions are as follows:

1) The increase in the rotation speed of the inner ring causes the temperature of each component to increase, and the temperature of the ball contact area increases the most. As the revolution speed of the ball is smaller than that of the inner ring, the angular velocity of the outer ring relative to the ball is quite small. Hence, the outer ring is less affected by frictional heat generation than the inner ring and ball. Therefore, the temperature rise of the outer ring contact area is smaller than that of the inner ring.

2) The increase in the rotation speed of the inner ring causes the axial deformation of the inner ring to increase, that is, the dynamic stiffness of the bearing decreases with the increase of the rotation speed. This condition affects the high-speed running state and accuracy of the bearing and further influences the running state of the high-speed spindle system of the machine tool.

Acknowledgments

This work is supported by the National Key Research and Development Program, China (2018YFB2000202).

Nomenclature

M : Mass
C : Damping
K : Stiffness
P : Load
$C(T)$: Specific heat
$K(T)$: Heat transfer
$Q(T)$: Heat flow load
u : Displacement
T : Temperature
ω_m : Rotation angular velocity of ball
D_b : Diameter of ball
d_m : Pitch diameter
α_i : Contact angle of ball with inner raceway
α_o : Contact angle of ball with outer raceway
ω : Angular velocity of inner ring
$\boldsymbol{\tau}$: Frictional stress
$\dot{\gamma}$: Slip rate
P_f : Friction energy dissipation rate
q : Friction heat
f : Proportion of frictional heat flowing into the first surface
η : Coefficient of conversion of mechanical energy into thermal energy
k : Thermal conductivity of lubricant
P_r : Prandtl number of lubricant
R_e : Reynolds number
u_s : Surface speed of cage
v_0 : Kinematic viscosity of lubricating oil
T_a : Ambient temperature
k_a : Thermal conductivity of air
D_o : Outer diameter of bearing
u_a : Flow velocity of air
v_a : Kinematic viscosity of air

References

[1] Q. Han, X. Li and F. L. Chu, Skidding behavior of cylindrical roller bearings under time-variable load conditions, *International Journal of Mechanical Science*, 135 (1) (2018) 203-214.
[2] Q. Han, Z. Ding, X. Xu, T. Wang and F. Chu, Stator current model for detecting rolling bearing faults in induction motors

using magnetic equivalent circuits, *Mechanical Systems and Signal Processing*, 131 (1) (2019) 554-575.
[3] Q. Han, Z. Ding, Z. Qin, T. Wang, X. Xu and F. Chu, A triboelectric rolling ball bearing with self-powering and self-sensing capabilities, *Nano Energy*, 67 (1) (2020) 104277.
[4] N. Song, *Analysis on Temperature Field and Thermo-stress Coupling of High Speed Angular Contact Ball Bearing with Spin Heat Generation*, Jilin University, Jilin, China (2017).
[5] T. A. Harris and M. N. Kotzalas, *Advanced Concepts of Bearing Technology*, 5th Ed., CRC Press, Boca Raton, USA (2006).
[6] A. Tedric and M. N. K. Harris, *Essential Concepts of Bearing Technology*, 5th Ed. CRC Press, Boca Raton, USA (2007).
[7] A. Palmgren, *Ball and Roller Bearing Engineering*, 4th Ed., S. H. Burbank, Philadelphia (1959).
[8] Z. De-xing, C. Weifang and L. Miaomiao, An optimized thermal network model to estimate thermal performances on a pair of angular contact ball bearings under oil-air lubrication, *Applied Thermal Engineering*, 131 (1) (2018) 328-339.
[9] D. Zheng and W. Chen, Thermal performances on angular contact ball bearing of high-speed spindle considering structural constraints under oil-air lubrication, *Tribology International*, 109 (1) (2017) 593-601.
[10] D. Zheng, W. Chen and M. Li, An improved model on forecasting temperature rise of high-speed angular contact ball bearings considering structural constraints, *Industrial Lubrication and Tribology*, 70 (1) (2018) 15-22.
[11] J. Takabi and M. M. Khonsari, Experimental testing and thermal analysis of ball bearings, *Tribology International*, 60 (1) (2013) 93-103.
[12] P. He, F. Gao, Y. Li, W. Wu and D. Zhang, Study on thermo-mechanical coupling characteristics of angle contact ball bearing with fix-position preload, *Industrial Lubrication and Tribology*, 71 (1) (2019) 795-802.
[13] K. Yan, J. Hong, J. Zhang, W. Mi and W. Wu, Thermal-deformation coupling in thermal network for transient analysis of spindle-bearing system, *International Journal of Thermal Sciences*, 104 (1) (2016) 1-12.
[14] A. Zahedi and M. R. Movahhedy, Thermo-mechanical modeling of high speed spindles, *Scientia Iranica*, 19 (2) (2012) 282-293.
[15] H. Wang, Y. Cai and H. Wang, A dynamic thermal-mechanical model of the spindle-bearing system, *Mechanical Sciences*, 8 (2) (2017) 277-288.
[16] Z. Ye, L. Wang, G. Chen and D. Tang, Analysis of thermo-mechanical coupling of high-speed angular-contact ball bearings, *Advances in Mechanical Engineering*, 9 (6) (2017) 1-14.
[17] V. Than, C. Wang, T. Ngo and J. H. Huang, Estimating time-varying heat sources in a high speed spindle based on two measurement temperatures, *International Journal of Thermal Sciences*, 111 (1) (2017) 50-65.
[18] L. Cui, C. Cai and Q. Wang, Multi-objective optimization design algorithm of dynamic and thermal performances of high speed spindle bearing, *2016 IEEE Information Technology, Networking, Electronic and Automation Control Conference* (2016) 1001-1004.
[19] B. Yan, K. Yan, P. Zhang and Y. Zhu, Numerical simulation on the stress distribution of high speed angular contact rolling bearing, *2017 IEEE 7th Annual International Conference on CYBER Technology in Automation, Control, and Intelligent Systems (CYBER)* (2017) 317-320.
[20] B. Yan, K. Yan, T. Luo, Y. Zhu, B. Q. Li and J. Hong, Thermal coefficients modification of high speed ball bearing by multi-object optimization method, *International Journal of Thermal Sciences*, 137 (1) (2019) 313-324.
[21] C. Ma, X. Mei, J. Yang, L. Zhao and H. Shi, Thermal characteristics analysis and experimental study on the high-speed spindle system, *The International Journal of Advanced Manufacturing Technology*, 79 (4) (2015) 469-489.
[22] J. Huang, V. Than, T. Ngo and C. Wang, An inverse method for estimating heat sources in a high speed spindle, *Applied Thermal Engineering*, 105 (1) (2016) 65-76.
[23] P. Huang, *Numerical Calculation Methods of Elastohydrodynamic Lubrication*, 1st Ed., Tsinghua University Press, Beijing, China (2013).
[24] H. Xu, *Numerical Simulation and Optimization Design of Heavy Load Rolling Bearings*, 1st Ed., Tsinghua University Press, Beijing, China (2010).

Lanwen Wang is a Ph.D. student in Department of Mechanical Engineering, Tsinghua University, Beijing, China. He received his B.E. degree in Shandong University (2019). His research interests include friction, heat transfer and lubrication of bearing.

Xuanyu Sheng is an Associate Professor in Department of Mechanical Engineering, Tsinghua University, Beijing, China. He received his Ph.D. in Tsinghua University (1998). His research interests include friction properties analysis of materials, structural design, seismic analysis and simulation.